Human Reproduction, Vol.36, No.7, pp. 1891–1906, 2021
Advance Access Publication on June 1, 2021 doi:10.1093/humrep/deab135

human reproduction

ORIGINAL ARTICLE ***Reproductive biology***

Hypo-glycosylated hFSH drives ovarian follicular development more efficiently than fully-glycosylated hFSH: enhanced transcription and PI3K and MAPK signaling

Guohua Hua [1,2], Jitu W. George[2,3], Kendra L. Clark[2,3], Kim C. Jonas[4], Gillian P. Johnson [4], Siddesh Southekal[5], Chittibabu Guda[5], Xiaoying Hou[2], Haley R. Blum[2], James Eudy[5], Viktor Y. Butnev[6], Alan R. Brown[6], Sahithi Katta[6], Jeffrey V. May[6], George R. Bousfield [6], and John S. Davis [2,3,*]

[1]Key Lab of Agricultural Animal Genetics, Breeding and Reproduction of Ministry of Education, College of Animal Science & Technology, Huazhong Agricultural University, Wuhan, Hubei, China [2]Department of Obstetrics and Gynecology, Olson Center for Women's Health, University of Nebraska Medical Center, Omaha, NE, USA [3]Veterans Affairs Nebraska Western Iowa Health Care System, Omaha, NE, USA [4]Department of Women and Children's Health, School of Life Course Sciences, King's College London, Guy's Campus, London, UK [5]Department of Genetics, Cell Biology and Anatomy, University of Nebraska Medical Center, Omaha, NE, USA [6]Department of Biological Sciences, Wichita State University, Wichita, KS, USA

*Correspondence address. Department of Obstetrics and Gynecology, Olson Center for Women's Health, University of Nebraska Medical Center, Omaha, NE 68198, USA. E-mail: jsdavis@unmc.edu https://orcid.org/0000-0003-3468-4079

Submitted on August 24, 2020; resubmitted on March 31, 2021; editorial decision on May 04, 2021

STUDY QUESTION: Does hypo-glycosylated human recombinant FSH (hFSH18/21) have greater *in vivo* bioactivity that drives follicle development *in vivo* compared to fully-glycosylated human recombinant FSH (hFSH24)?

SUMMARY ANSWER: Compared with fully-glycosylated hFSH, hypo-glycosylated hFSH has greater bioactivity, enabling greater follicular health and growth *in vivo*, with enhanced transcriptional activity, greater activation of receptor tyrosine kinases (RTKs) and elevated phosphatidylinositol 3-kinase (PI3K)/protein kinase B (AKT) and Mitogen-activated protein kinase (MAPK)/extracellular signal-regulated kinase (ERK) signaling.

WHAT IS KNOWN ALREADY: Glycosylation of FSH is necessary for FSH to effectively activate the FSH receptor (FSHR) and promote preantral follicular growth and formation of antral follicles. *In vitro* studies demonstrate that compared to fully-glycosylated recombinant human FSH, hypo-glycosylated FSH has greater activity in receptor binding studies, and more effectively stimulates the PKA pathway and steroidogenesis in human granulosa cells.

STUDY DESIGN, SIZE, DURATION: This is a cross-sectional study evaluating the actions of purified recombinant human FSH glycoforms on parameters of follicular development, gene expression and cell signaling in immature postnatal day (PND) 17 female CD-1 mice. To stimulate follicle development *in vivo*, PND 17 female CD-1 mice (n = 8–10/group) were treated with PBS (150 µl), hFSH18/21 (1 µg/150 µl PBS) or hFSH24 (1 µg/150 µl PBS) by intraperitoneal injection (i.p.) twice daily (8:00 a.m. and 6:00 p.m.) for 2 days. Follicle numbers, serum anti-Müllerian hormone (AMH) and estradiol levels, and follicle health were quantified. PND 17 female CD-1 mice were also treated acutely (2 h) *in vivo* with PBS, hFSH18/21 (1 µg) or hFSH24 (1 µg) (n = 3–4/group). One ovary from each mouse was processed for RNA sequencing analysis and the other ovary processed for signal transduction analysis. An *in vitro* ovary culture system was used to confirm the relative signaling pathways.

PARTICIPANTS/MATERIALS, SETTING, METHODS: The purity of different recombinant hFSH glycoforms was analyzed using an automated western blot system. Follicle numbers were determined by counting serial sections of the mouse ovary. Real-time quantitative RT-PCR, western blot and immunofluorescence staining were used to determine growth and apoptosis markers related with follicle health.

RNA sequencing and bioinformatics were used to identify pathways and processes associated with gene expression profiles induced by acute FSH glycoform treatment. Analysis of RTKs was used to determine potential FSH downstream signaling pathways *in vivo*. Western blot and *in vitro* ovarian culture system were used to validate the relative signaling pathways.

MAIN RESULTS AND THE ROLE OF CHANCE: Our present study shows that both hypo- and fully-glycosylated recombinant human FSH can drive follicular growth *in vivo*. However, hFSH18/21 promoted development of significantly more large antral follicles compared to hFSH24 ($P < 0.01$). In addition, compared with hFSH24, hFSH18/21 also promoted greater indices of follicular health, as defined by lower BAX/BCL2 ratios and reduced cleaved Caspase 3. Following acute *in vivo* treatment with FSH glycoforms RNA-sequencing data revealed that both FSH glycoforms rapidly induced ovarian transcription *in vivo*, but hypo-glycosylated FSH more robustly stimulated Gαs and cAMP-mediated signaling and members of the AP-1 transcription factor complex. Moreover, hFSH18/21 treatment induced significantly greater activation of RTKs, PI3K/AKT and MAPK/ERK signaling compared to hFSH24. FSH-induced indices of follicle growth *in vitro* were blocked by inhibition of PI3K and MAPK.

LARGE SCALE DATA: RNA sequencing of mouse ovaries. Data will be shared upon reasonable request to the corresponding author.

LIMITATIONS, REASONS FOR CAUTION: The observations that hFSH glycoforms have different bioactivities in the present study employing a mouse model of follicle development should be verified in nonhuman primates. The gene expression studies reflect transcriptomes of whole ovaries.

WIDER IMPLICATIONS OF THE FINDINGS: Commercially prepared recombinant human FSH used for ovarian stimulation in human ART is fully-glycosylated FSH. Our findings that hypo-glycosylated hFSH has greater bioactivity enabling greater follicular health and growth without exaggerated estradiol production *in vivo*, demonstrate the potential for its development for application in human ART.

STUDY FUNDING/COMPETING INTEREST(S): This work was supported by NIH 1P01 AG029531, NIH 1R01 HD 092263, VA I01 BX004272, and the Olson Center for Women's Health. JSD is the recipient of a VA Senior Research Career Scientist Award (1IK6 BX005797). This work was also partially supported by National Natural Science Foundation of China (No. 31872352). The authors declared there are no conflicts of interest.

Key words: fertility/ FSH/ gonadotropin action/ ovary/ follicle development/ assisted reproduction/ transcription/ granulosa cell/ cell signaling/ glycosylation

Introduction

Ovarian follicles are the functional ovarian units responsible for ovum maturation and sex steroid hormone production. The follicle consists of an outer layer of theca interstitial cells, a basement membrane and multiple layers of granulosa cells that surround the ovum. Follicular growth can be divided into three stages (i) gonadotropin-independent (primordial, primary and secondary follicles), (ii) gonadotropin-responsive (transition from the preantral to early antral follicles) and (iii) gonadotropin-dependent (beyond the early antral stage) (Orisaka *et al.*, 2009). The pituitary gonadotropin, FSH, is required for antral follicular development and maturation (Allan *et al.*, 2006; McDonald *et al.*, 2019). FSH binds to and activates its receptor, FSH receptor (FSHR) (Ulloa-Aguirre *et al.*, 2018), located on granulosa cells to promote growth and survival signaling events that result in estrogen production and granulosa cell proliferation, promoting the growth of antral follicles (George *et al.*, 2011). FSH also orchestrates granulosa cell differentiation, priming the follicle to respond to endocrine and paracrine signals that result in ovulation of a mature oocyte.

FSH is a heterodimeric glycoprotein hormone possessing 4 asparagine (N)-linked, glycosylation sites: Asn^{52} and Asn^{78} in the FSHα subunit and Asn^{7} and Asn^{24} in the FSHβ subunit (Bousfield and Harvey, 2019). Recent studies have identified several different FSH glycoforms based on the location of one or two glycans in their FSHβ subunit, because the FSHα subunit invariably possesses both Asn^{52} and Asn^{78} N-glycans. Fully-glycosylated FSH (FSH24) (based on FSHβ molecular weight determinations) possesses N-glycans attached to both Asn^{7} and Asn^{24} residues; whereas partially glycosylated FSH21 possesses only the β-subunit Asn^{7} glycan; and partially glycosylated FSH18 possesses only the β-subunit Asn^{24} glycan (Davis *et al.*, 2014; Bousfield *et al.*, 2018). Previous studies demonstrated that chemical de-glycosylation of FSH adversely influenced its bioactivity and circulatory half-life (Meher *et al.*, 2015). Recent evidence suggests that the human pituitary synthesizes and secretes multiple FSH glycoforms and FSH glycoform abundance is under physiological regulation (Walton *et al.*, 2001; Bousfield *et al.*, 2014b). The pituitaries of young women contain predominately hypo-glycosylated FSH, while FSH24 predominates in pituitaries of postmenopausal women, due to a decrease in the abundance of hypo-glycosylated FSH21 (Bousfield *et al.*, 2007). Fully-glycosylated FSH24 is also the most abundant glycoform in postmenopausal urinary human recombinant FSH (hFSH) preparations and in recombinant hFSH preparations used clinically in ART approaches for controlled ovarian stimulation (Bousfield *et al.*, 2007, 2014b; Butnev *et al.*, 2015).

Hypo-glycosylated FSH was reported to be more active compared with fully-glycosylated FSH24 in several receptor binding assays (Bousfield *et al.*, 2014a). Utilizing the KGN human granulosa cell line, our group demonstrated that hypo-glycosylated FSH glycoforms (FSH18/21) exhibited significantly greater ability to stimulate cAMP- and protein kinase A (PKA)-dependent signaling, as well as estrogen and progesterone synthesis, compared with fully-glycosylated FSH (FSH24) (Jiang *et al.*, 2015). Very recent studies verified that FSH18/21 was more bioactive in primary cultures of porcine granulosa cells (Liang *et al.*, 2020) and HEK293 cells expressing the human FSHR (Zariñán *et al.*, 2020). In studies employing the FSHβ subunit null mouse (*Fshb* null), both hypo- and fully-glycosylated FSH were able rescue ovarian weight loss and promote antral follicle formation (Wang *et al.*, 2016). Furthermore, *in vitro* culture of secondary follicles

isolated from pre-pubertal mice showed that both FSH glycoforms were able to stimulate PKA and FSH-responsive gene expression (Simon *et al.*, 2019).

Recombinant hFSH preparations administered to patients undergoing ART protocols are similar to fully-glycosylated FSH isoforms observed in postmenopausal pituitaries and urine (Daya and Gunby, 1999). Women of advanced reproductive age often respond poorly to FSH or require multiple ART cycles with increasing doses of FSH (van Rooij *et al.*, 2003). Despite studies indicating that FSH18/21 is more efficient than FSH24 *in vitro*, the clearance of FSH18/21 and FSH24, and the bioactivity of differentially glycosylated recombinant hFSH glycoforms on folliculogenesis *in vivo*, as well as their downstream signaling pathways and target gene networks remain to be described.

In the present study, we employed *in vivo* and *in vitro* experimental mouse models to evaluate the actions of recombinant hFSH glycoform preparations on ovarian signaling pathways, transcriptomic profiles and follicular development. Although, both hypo-glycosylated FSH and fully-glycosylated FSH stimulated follicular development, FSH18/21 treatment resulted in greater numbers of large antral follicles. Compared to FSH24, FSH18/21 more effectively activated multiple receptor tyrosine kinase (RTK)-, phosphatidylinositol 3-kinase (PI3K)/protein kinase B (AKT) and Mitogen-activated protein kinase (MAPK)/extracellular signal-regulated kinase (ERK) signaling pathways that are crucial for follicle growth and survival. Analysis of the ovarian transcriptome using RNA sequencing revealed that FSH18/21 induced a more robust expression of early response genes, including members of the *Fos* and *Jun* AP-1 transcription family, nuclear receptor 4a (*Nr4a*) family, and early growth response (*Egr*) family. The current findings indicate that hypo-glycosylated FSH (hFSH18/21) has greater bioactivity compared to fully-glycosylated FSH (hFSH24) in a functional mouse model *in vivo*.

Materials and methods

Chemicals and reagents

The production, purification and characterization of recombinant fully-glycosylated FSH and hypo-glycosylated FSH glycoforms were described previously (Butnev *et al.*, 2015) and glycoform analysis and clearance studies are described in Supplementary Methods. The RNeasy Mini Kit was from Qiagen (Hilden, Germany). qRT-PCR reagents and RT-PCR reagents were from BioRad (Hercules, CA, USA). Primary and secondary antibodies used for western-blotting or immunofluorescent staining are listed in Supplementary Table SI.

Ovarian histology and serial follicle counting

The prepubertal mouse model (17 day postnatal, PND17), which minimizes endogenous FSH was selected for use in this study. After birth, the endogenous plasma concentrations of FSH decline at 15 dpn and are maintained at a very low level until puberty (Michael *et al.*, 1980). The hypothalamic–pituitary–gonadal axis is established in immature mice at 2–3 weeks (Glanowska *et al.*, 2014). Treatment of immature mice (PND 14–17) with a GnRH receptor antagonist Ganirelix shows significant decreases in endogenous FSH levels but no alterations in follicular growth compared with controls (Francois *et al.*, 2017), indicating that endogenous FSH has minor effect on follicular development at this period. Importantly, numerous follicles develop to the preantral/early antral stage and ovarian FSH receptivity increases rapidly during this period, emphasizing that growing follicles become sensitive to gonadotropins (Francois *et al.*, 2017). Collectively, these studies indicated that the prepubertal mouse model (17 dpn), which minimizes the endogenous FSH, is a reliable model to evaluate the effects of exogenous hypo- and fully-glycosylated FSH on the follicular development.

To stimulate follicle development female CD-1 mice (PND 17) were treated with PBS (150 µl), hFSH18/21 (1 µg/150 µl PBS) or hFSH24 (1 µg/150 µl PBS) by intraperitoneal injection (i.p.) twice daily (8:00 a.m. and 6:00 p.m.) for 2 days. All mice were euthanized 48 h after the first injection and ovaries were isolated. One ovary from each mouse was immediately frozen in liquid nitrogen for subsequent extraction of protein or RNA. The other ovary was immediately fixed in modified Davidson's fixative (Newcomer Supply, Middleton, WI, USA) for 4–6 h and processed for paraffin embedding with a protocol established in our laboratory (Lv *et al.*, 2019). The samples were dehydrated, embedded in paraffin, and 5 µm serial sections were cut. Sections were placed in order onto positively charged glass slides followed by Hematoxylin and Eosin staining (HE). Secondary, small antral, and large antral follicles were counted in every 5th serial section. Only follicles containing a clearly stained oocyte nucleus were counted.

Fluorescent immunohistochemistry

Fluorescence immunohistochemistry was used to determine the expression and localization of cell fate makers, Ki67 and cleaved Caspase 3 proteins, in mouse ovary sections. The paraffin sections, and the immunostaining for Ki67, cleaved Caspase 3 proteins were performed as described before (Hua *et al.*, 2016). Slides were mounted by adding Vectashield Vibrance Antifade mounting medium with DAPI (Vector Laboratories, Inc., Burlingame, CA, USA). Images were captured using a Zeiss 800 Meta Confocal Laser Scanning Microscope and analyzed using Zeiss Zen 3.0 software (Carl Zeiss, Oberkochen, Germany).

AMH and estradiol measurements

Mice were euthanized and blood was collected, centrifuged, and the serum was stored at −80°C. Measurements of AMH and estradiol were performed at the Center for Research in Reproduction Ligand Assay and Analysis Core, University of Virginia.

RNA sequencing

Postnatal day (PND) 17 female CD-1 mice were treated i.p. with PBS (150 µl), hFSH18/21 (1 µg/150 µl PBS) or hFSH24 (1 µg/150 µl PBS). Ovaries were isolated 2 h after treatment and stored at −80°C. Total RNA was extracted using RNeasy mini kit (QIAGEN) and subjected to DNAase treatment using the RNase-Free DNase Set (QIAGEN) according to the manufacturer's instructions. RNA purity and integrity were tested and scored between 8.3 and 10. RNA libraries were prepared using the TruSeq V2 kit (Illumina). Libraries were sequenced on the NextSeq550 on a high-output, 75 bp paired-end flow cell, at the University of Nebraska Medical Center Genomics Core facility. The software and details for RNA sequencing data bioinformatics analysis are described in the Supplementary Methods.

Quantitative RT-PCR analysis

RNA-Sequencing data were confirmed by quantitative RT-PCR (qRT-PCR). Reverse transcription was completed using iScript Reverse Transcription Supermix (BioRad, Hercules, CA, USA). qRT-PCR was performed on a BioRad CFX96™ Real-Time System (Bio-Rad Laboratories, Inc., Hercules, CA) based on a protocol established in our laboratory (Hua *et al.*, 2016). qRT-PCR primers were designed using Primerbank online software (https://pga.mgh.harvard.edu/primerbank/) and commercially synthesized by Dharmacon™ Inc. (Lafayette, CO, USA). The primer sequences are listed in Supplementary Table SII.

Receptor tyrosine kinases analysis

RTK arrays were used to analyze potential FSH downstream signaling pathways *in vivo*. PND 17 female CD-1 mice (5 mice/group) were treated i.p. with PBS (150 µl), hFSH18/21 (1 µg/150 µl PBS) or hFSH24 (1 µg/150 µl PBS). Mice were euthanized 2 h after injection. Ovaries were rapidly isolated and placed into liquid nitrogen. The Proteome Profiler Mouse Phospho-RTK Array Kit (Cat.: ARY014, R&D Systems) was used to determine the relative tyrosine phosphorylation levels of 39 RTKs according to the manufacturer's protocol. The intensities of different tyrosine phosphorylations were quantitated by VisionWorks Image Acquistition and Analysis software (Upland, CA, USA). The relative intensities of the averaged signal from each pair of duplicated spots were normalized to control spots in each array.

Western blot analysis

Ovaries harvested from control, hFSH18/21 or hFSH24 treatment groups were homogenized in RIPA buffer. Protein concentrations were measured by Bio-Rad protein assay (Bio-Rad, CA, USA). Western blotting and quantification were performed based on a protocol established in our laboratory (Plewes *et al.*, 2019).

In vitro culture of mouse ovaries

Whole ovaries were collected from CD-1 female mice aged 3 to 5 weeks (Harlan, Shardlow, UK). Mice were housed in accordance with the Animals (Scientific Procedures) Act of 1986 and associated Codes of Practice, with 12-h light/dark cycle and ad libitum access to standard chow and water. Once removed, ovaries were dissected into four equal parts in Liebovitz L15 medium (Life Technologies, Paisley, UK) supplemented with 1% (w/v) bovine serum albumin (Sigma, Aldrich, St Louis, MO, USA). Ovary sections were then transferred into a single well of a 24-well plate (one section per well) containing 500 µL Minimal Essential Medium alpha (MEM-α, Life Technologies, Paisley, UK) supplemented with 0.1% (w/v) bovine serum albumin, 75 mg/mL penicillin (Sigma, Aldrich, St Louis, MO, USA), 100 mg/mL streptomycin sulfate (Sigma, Aldrich, St Louis, MO, USA), and a cocktail of 5 mg/mL insulin, 5 mg/mL transferrin and 5 ng/mL sodium selenite (ITS; Sigma, Aldrich, St Louis, MO, USA). Ovary sections were incubated at 37°C in a humidified incubator in 5% CO_2 in air. Ovary sections were pre-treated with either media alone containing vehicle (0.1% (v/v) DMSO), 100 nM Wortmannin (PI3K inhibitor) or 10 µM U0126 (MEK inhibitor) for 60 min. Following pre-treatment, ovarian sections were treated with media alone (control), 30 ng/ml FSH18/21 or FSH24 in the presence or absence of vehicle, 100 nM Wortmannin or 10 µM U0126 for 48 h. At the end of the culture period, the ovary sections were snap frozen in dry ice.

Ovary sections were mechanically disrupted using a battery-operated pestle motor and lysed with TRI Reagent® (93289; Sigma Aldrich, St Louis, MO, USA). mRNA was extracted as per the manufacturer's protocol. The concentration of RNA in each sample was measured using a Nanodrop spectrophotometer and 400 ng of RNA was reverse transcribed to cDNA using the High-Capacity cDNA Reverse Transcription Kit (Applied Biosystems, Foster City, CA, USA). Quantitative RT-PCR (qRT-PCR) was performed using a 10 µl reaction mix containing 5 µl QuantiFast SYBR Green PCR Kit (Qiagen, Germany), 0.4 µl of each primer, and 4.2 µl of sample and H_2O mix. Plates were run in an ABI 7500 Fast Real-Time PCR machine (Life Technologies, Carlsbad, CA, USA). The cycle parameters were as follows: Uracil N-glycosylase (UNG) activation was run for 2 min at 50°C, DNA polymerase activation for 5 min at 95°C, the melt cycle was run for 10 s at 95°C and the annealing–extending cycle for 30 s at 60°C. A no-template control was run in each 384-well plate to confirm the absence of contamination. Each sample was normalized to reference gene *Rpl-19* and to no treatment control using relative quantification method. All primer sequences and concentrations are outlined in Supplementary Table SII. The relative expression of each gene was normalized to expression of *Rpl-19*, normalized as fold-change in gene expression relative to the control group.

Statistical analysis

Statistical analyses were conducted using GraphPad Prism software (GraphPad Software, LLC.). Following normality testing, parametric or non-parametric testing was performed using one-way ANOVA with subsequent multiple range tests. Data are presented as means ± SEM.

Study approval

Female CD-1 mice were purchased from Charles River laboratories (MA, USA). All mice were maintained under 12 h dark and 12 h light cycles with food and water supplied *ad libitum* at University of Nebraska Medical Center animal facility. The animal handling procedures and all experimental protocols were approved by the Institutional Animal Care and Use Committee at the University of Nebraska Medical Center.

Results

FSH glycoforms used in this study compared to gonal-f®

Gonal-f® (follitropin alfa for injection) is a commercial FSH preparation of recombinant DNA origin, which is employed therapeutically to induce ovarian follicular development in human ARTs (Saz-Parkinson *et al.*, 2009). To identify the glycoforms of hypo- and fully-glycosylated recombinant FSH, an automated western blot system was employed to analyze different FSH preparations. Recombinant hFSH glycoforms were compared with a pituitary hFSH reference (for FSHβ variant mobilities only) and Gonal-f® (Fig. 1a). Automated western blot results showed that Gonal-f® possessed 95% 24 kDa hFSHβ. For hypo-glycosylated recombinant FSH (FSH18/21), 89% migrated as 18 and 11% as

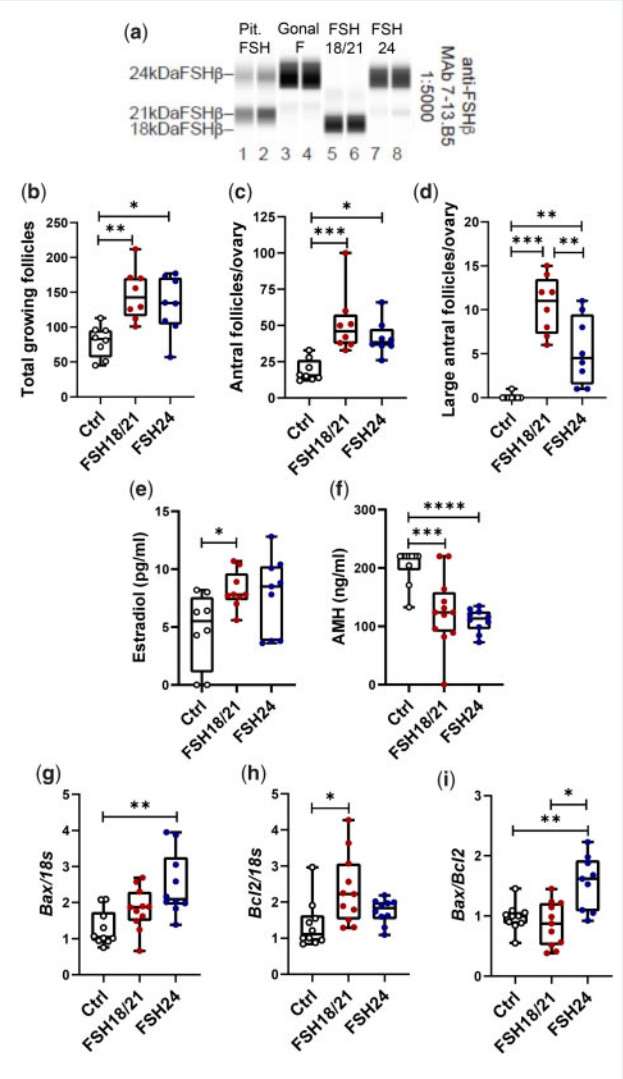

Figure 1. The effects of hypo- and fully-glycosylated human recombinant FSH (hFSH) on follicular development *in vivo*. (**a**) Automated western blot of recombinant hFSH preparations. The primary FSHβ antibody was 7-13.B5 diluted 1:5000. Lanes 1 and 2, 100 ng pituitary FSH AFP7298A; lanes 3 and 4, 100 ng Gonal-f® (FSH used in clinical ART); lanes 5 and 6, 100 ng hFSH18/21; lanes 7 and 8, 100 ng hFSH24. (**b**) Total growing follicles, including pre-antral follicles, and antral follicles, 48 h after treatment with hFSH18/21 and hFSH24. (**c**) Numbers of antral follicles per ovary in control, hFSH18/21 and hFSH24 treatment groups. (**d**) Number of large antral follicles per ovary in control, hFSH18/21 and hFSH24 treatment groups. (**e**) Serum estradiol concentrations (pg/ml) in different treatment groups. (**f**) Serum anti-Müllerian hormone (AMH) concentrations (ng/ml) in different treatment groups. (**g–i**) Total RNA was extracted for qRT-PCR in Control, hFSH18/21, and hFSH24 treatment groups. (**g**) Ovarian transcripts for *Bax*. (**h**) Ovarian transcripts for *Bcl2*. (**i**) *Bax* versus *Bcl2* gene expression ratio. *$P < 0.05$; **$P < 0.01$; ***$P < 0.001$; ****$P < 0.0001$.

21 kDa hFSHβ. Fully-glycosylated recombinant FSH was comprised of 91% 24 kDa hFSHβ. These results demonstrate that the widely used recombinant hFSH formulation is similar to fully-glycosylated FSH (FSH24).

Recombinant hFSH18/21 has greater bioactivity than hFSH24 in stimulating *in vivo* follicle development

Because FSH is required for antral follicular development *in vivo*, we performed experiments to evaluate the response to different FSH glycoforms using pre-pubertal CD-1 mice, which have low levels of endogenous FSH (Michael *et al.*, 1980). Treatment of PND 17 mice with either hypo-glycosylated FSH (hFSH18/21) or fully-glycosylated FSH (hFSH24) for 48 h resulted in a significant increase in follicle development (Supplementary Fig. S1). Treatment with hFSH18/21 or hFSH24 induced similar numbers of growing follicles and antral follicles (Fig. 1b, 1c). Interestingly, hFSH18/21 treatment resulted in a two-fold increase in numbers of large antral follicles when compared to hFSH24 ($P < 0.01$, Fig. 1d). Analysis of circulating hormone concentrations revealed that both FSH18/21 and FSH24 treatment increased estradiol ($P < 0.05$) when compared with control (Fig. 1e). Both FSH glycoforms suppressed AMH when compared with the control group ($P < 0.001$), but no differences were found between the treatment groups (Fig. 1f).

Follicles exhibiting apoptosis in a large portion of mural granulosa cells are likely undergoing atresia (Regan *et al.*, 2018). Follicles yielding oocytes that fertilized have low levels of granulosa cell apoptosis, while follicles from patients with poor oocytes have greater levels of apoptosis markers (Nakahara *et al.*, 1997; Oosterhuis *et al.*, 1998). To determine whether hFSH18/21 and hFSH24 differentially affected follicular health, we measured the expression of transcripts for two Bcl-2 family members, *Bax* and *Bcl2*, which either promote or inhibit apoptosis, respectively. The *Bax*/*Bcl-2* ratio acts as a rheostat that determines susceptibility to apoptosis (Raisova *et al.*, 2001; Hsueh *et al.*, 2015). Transcripts for the pro-apoptosis activator *Bax* were upregulated in the hFSH24 treatment group ($P < 0.01$) (Fig. 1g), and transcripts for *Bcl2*, which prevents apoptosis, were upregulated in the hFSH18/21 treatment group ($P < 0.05$) (Fig. 1h). The ratio of *Bax*/*Bcl2* was increased significantly in the hFSH24 treatment group, suggesting a pro-apoptotic phenotype (Fig. 1i). Western blot data confirmed that the ratio of Bax to Bcl2 proteins was upregulated following hFSH24 treatment group (Fig. 2a and b). Transcripts for cyclin D (*Ccnd1*), a granulosa cell proliferation marker, were upregulated in the FSH18/21 treatment group (Fig. 2c), although no changes in levels of ovarian cyclin D protein were observed in either treatment group (Fig. 2d). The presence of Ki67 staining, as a marker of cell proliferation, confirmed that both hFSH18/21 and hFSH24 stimulated follicle growth *in vivo* (Fig. 2e and f). However, the apoptosis marker cleaved-Caspase 3 was more abundant in granulosa cells of mice treated with hFSH24 as compared with granulosa cells in the hFSH18/21 treatment group (Fig. 2g and h). Together with the findings shown in Fig. 1, these data support the idea that, while both FSH glycoforms promote follicle development, hFSH18/21 has more favorable actions on follicular health.

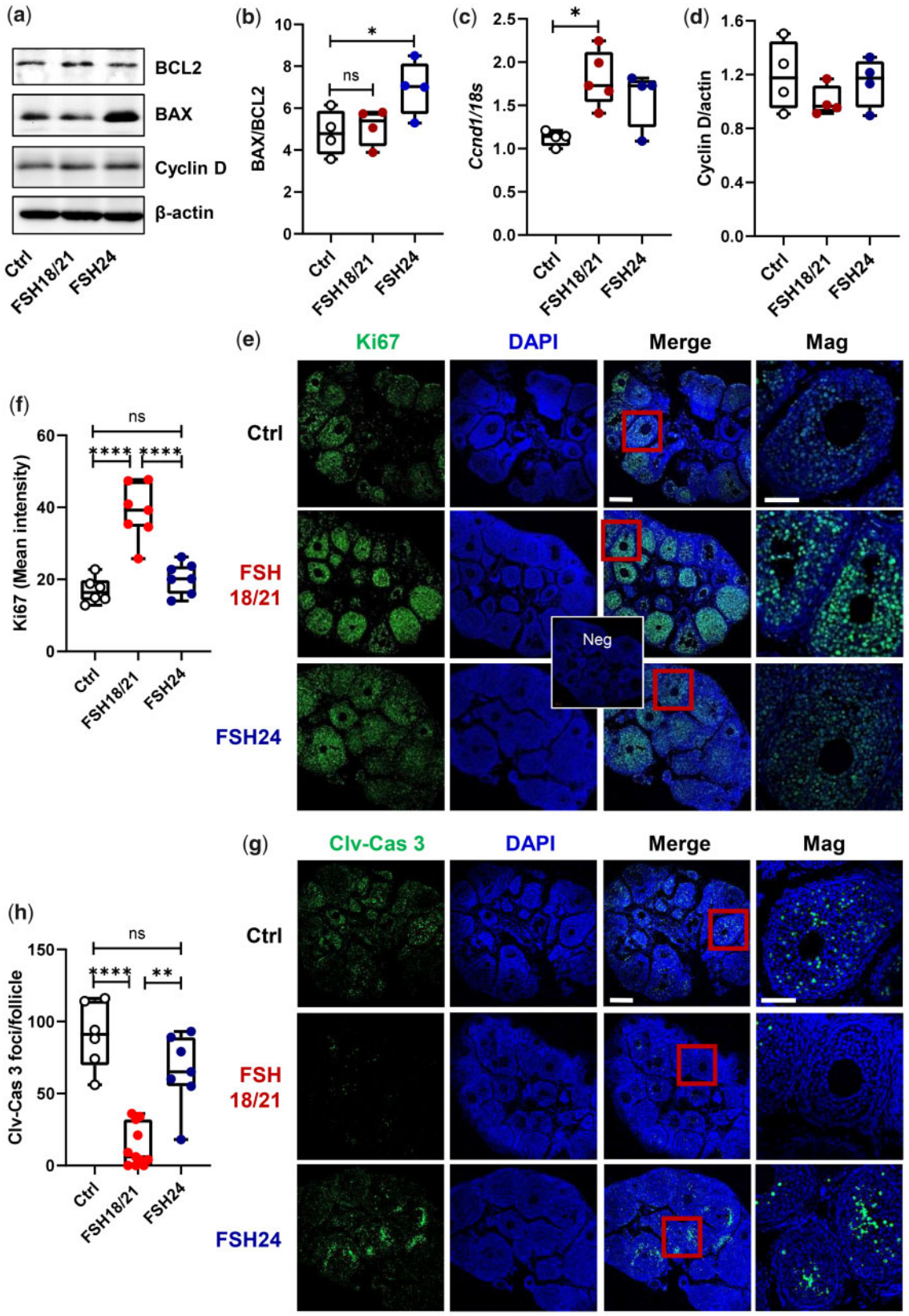

Figure 2. Apoptosis-related gene and protein expression in mouse ovaries. Mouse ovaries were isolated 48 h after PBS, hFSH18/21 or hFSH24 treatments. Total RNA and protein were extracted for qRT-PCR and western blot analysis. (**a**) Representative images of ovarian protein expression levels of Bcl2, Bax and Cyclin D detected by western blot. (**b**) Quantification data showing the Bax versus Bcl2 protein ratio. (**c**) Ovarian

Differential expression of genes in response to hFSH18/21 and hFSH24

Hypo-glycosylated hFSH was reported to exhibit 9∼20-fold higher FSHR binding activity compared with fully-glycosylated FSH (Bousfield *et al.*, 2014a). To better understand the actions of hypo- and fully-glycosylated FSH *in vivo*, we used PND 17 CD-1 mice as a model to explore ovarian transcriptomes in response to hFSH18/21 and hFSH24 treatment. Principal component analysis (PCA) of the gene expression data showed that hFSH18/21, hFSH24 and control (Fig. 3a) groups differentially clustered with Principal Component 1 (PC1) explaining 44.7% of variability, separating hFSH18/21 and hFSH24 treatments from the control group. Principal Component 2 (PC2) included 13.1% of the total variance dividing control and hFSH24 treatment groups from the hFSH18/21 group. A total of 411 genes were differentially expressed in the hFSH18/21 treatment group compared with controls ($P \leq 0.01$, abs(log2FC)$\geq$2); 62% (253) were upregulated and 38% (158) were downregulated (Fig. 3b and c). Interestingly, we observed approximately two-fold increase, a total of 878 genes, in differently expressed genes in the hFSH24 group compared to hFSH18/21 treated mice. When compared with control ($P \leq 0.01$, abs(log2FC)$\geq$2), the hFSH24 treatment group had 41% upregulated genes and 59% downregulated genes (Fig. 3b and c), an inverse trend compared to hFSH18/21 treated mice. Compared with the hFSH24 treatment group, 68 genes were upregulated, and 5 genes were downregulated in the FSH18/21 group (Fig. 3b). Among the differentially expressed genes (DEGs), FSH-responsive candidate genes were selected and validated by qRT-PCR, including *Cyp19a1*, *Egr1*, *Fos* and *Inhbb* (Supplementary Fig. S2).

A heatmap displaying the top 50 DEGs showing the highest variance across all the three groups is shown in Supplementary Fig. S3a. Ingenuity pathway analysis (IPA) was performed to understand the underlying molecular and cellular functions associated with the actions of hFSH18/21 and hFSH24 (Fig. 3d and Supplementary Fig. S3b). There were three common *Molecular and Cellular Functions* pathways enriched in both hFSH18/21 and hFSH24 treatment groups, including Cellular Movement, Cell-to-Cell Signaling, and Cellular Development. In addition to the three common pathways, cell cycle and gene expression signals pathway were ranked in the top 5 pathways in the FSH18/21 group. Cell death and survival and molecular transport pathways were enriched in the FSH24 group (Fig. 3d). The common upstream regulators of FSH18/21 and FSH24 treatment groups included forskolin, tetradecanoylphorbol acetate, and IL1B (Supplementary Fig. S3c). Additionally, CREB1 and TNF ranked in the top 5 of the FSH18/21 group, and bucladesine (a cAMP analog) and CG showed up in the FSH24 treatment group. To better understand the relationship between DEGs in the control and FSH glycoform treatment groups, the String database (https://string-db.org/) was used to construct an interaction network. A total of 77 nodes/genes and 189 interactions were included in the Protein–Protein Interaction (PPI) network generated by FSH18/21 treatment (degree > 2, indicated a high number of relevant hub genes in the network) (Supplementary Fig. S4). Analysis of DEGs following hFSH24 treatment revealed a PPI network containing 167 nodes and 493 interactions (Supplementary Fig. S5). Functional enrichment analysis using Cytoscape also showed the top GO Components, Functions, and Processes involved in hFSH18/21 (Supplementary Table SIII) and FSH24 (Supplementary Table SIV) treatments.

A total of 301 overlapping DEGs were found between hFSH18/21 vs Ctrl and hFSH24 vs Ctrl groups (Fig. 3c). To identify commonality between the two treatments versus control groups, we performed core analysis of the common 301 DEG's obtained in IPA (Supplementary Fig. S6). Overlay of the expression profile revealed the enriched top canonical pathways, upstream regulators, *Molecular and Cellular Functions*, and overlapping DEGs and genes known to be affected by FSHB in IPA (Supplementary Fig. S6a–d). Intriguingly, Actin Cytoskeleton Signaling, P70S6K signaling *etc.* were enriched in the top canonical pathways (Supplementary Fig. S6a); and Cellular Development, Cellular Growth and Proliferation, and Cell Death and Survival signaling pathways ranked top 3 in the *Molecular and Cellular Functions* category (Supplementary Fig. S6c).

Hypo-glycosylated recombinant FSH stimulates greater expression of early response genes

When comparing the response to FSH24 with that to FSH18/21, the top 50 DEGs included 47 (94%) upregulated and 3 downregulated genes (Supplementary Fig. S7). Of the top 5 *Molecular and Cellular Functions* identified by IPA, 3 were similar to those identified when comparing either hFSH18/21 or hFSH24 to controls (Fig. 3d and e). Cell growth and proliferation pathway and cell morphology functions were elevated in the FSH18/21 vs. FSH24 group (Fig. 3e). Analysis of the top 5 canonical pathways (absolute Z score > 3.0) with which common genes were involved revealed (i) cAMP mediated signaling, (ii) Gαs signaling, (iii) HMGB1, (iv) synaptic depression, and (v) white adipose tissue browning (Fig. 3f). To better understand the different actions of hFSH18/21 and hFSH24, we generated networks by overlapping log2FC of DEGs known to be affected by *FSHB* using the Path Explorer tool in IPA (Fig. 3g). The network analysis predicted differential activation of PI3K and MAPK signaling complexes. The modeling also shows that the transcription factors including AP1, FOS and NR4A1 were also significantly differentially regulated by hFSH18/21 ($P < 0.05$). Besides these, multiple transcripts for factors involved in

Figure 2. Continued
mRNA levels of *Ccnd* in Control, hFSH18/21 and hFSH24 treatment groups. (**d**) Quantification data showing the Cyclin D protein expression level. (**e**) Immunofluorescence staining of the proliferation marker Ki67 in mouse ovaries isolated 48 h after PBS (Ctrl), FSH18/21 and FSH24 treatment. Neg: Primary antibody negative control. (**f**) Quantification of Ki67 immunosignal intensity (n = 6 ovaries). (**g**) Immunofluorescence staining showing the apoptosis marker cleaved-Caspase 3 (Clv-Cas 3) in the ovaries. (**h**) Quantification of Clv-Cas 3 foci number (n = 6–11 ovaries). Scale bar: 200 µm. *$P < 0.05$; **$P < 0.01$; ****$P < 0.0001$.

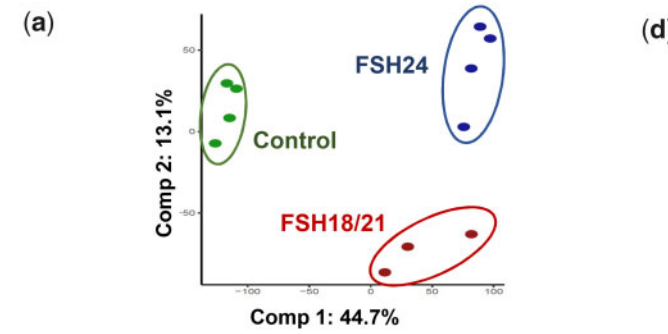

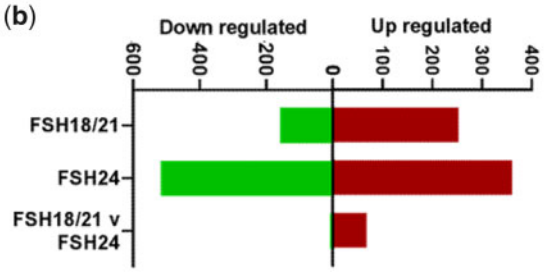

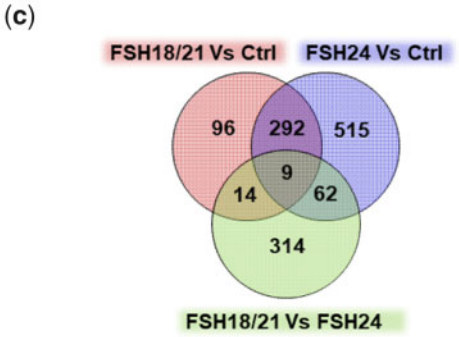

(d)

FSH18/21 Vs Control		
Name	P-value	# Mol.
Cellular Movement	3.10E-07 – 1.17E-26	249
Cell-To-Cell Signaling and Interaction	2.88E-07 – 3.26E-26	237
Cell Cycle	1.28E-07 – 1.95E-23	140
Gene Expression	1.28E-07 – 1.95E-23	219
Cellular development	3.09E-07 – 2.81E-23	297

FSH24 Vs Control		
Name	P-value	# Mol.
Cellular Movement	7.58E-07 – 1.30E-23	215
Cell-To-Cell Signaling and Interaction	7.72E-07 – 1.06E-21	201
Cell Death and Survival	7.63E-07 – 1.01E-19	261
Molecular Transport	7.50E-07 – 2.11E-17	231
Cellular development	6.67E-07 – 3.03E-20	290

(e)

FSH18/21 Vs FSH24		
Pathway	P-value	# Mol.
Cell-To-Cell Signaling and Interaction	7.14E-03 – 2.18E-09	209
Cellular development	7.14E-03 – 1.17E-05	69
Cell Growth and Proliferation	7.14E-03 – 1.17E-05	57
Molecular Transport	7.48E-03 – 1.50E-05	145
Cell Morphology	7.14E-03 – 3.18E-05	84

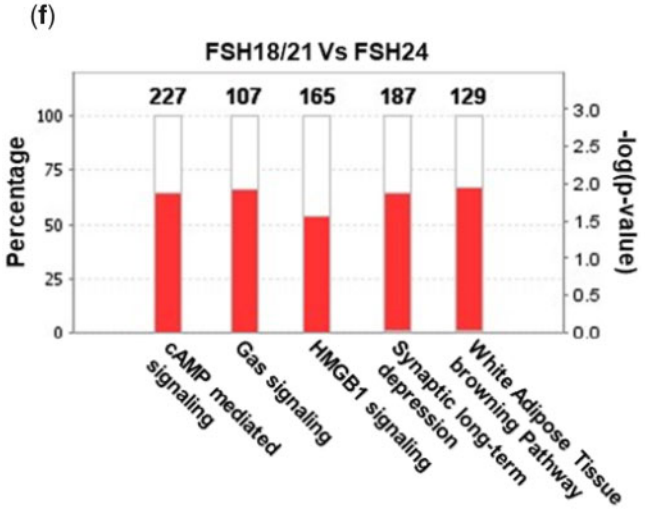

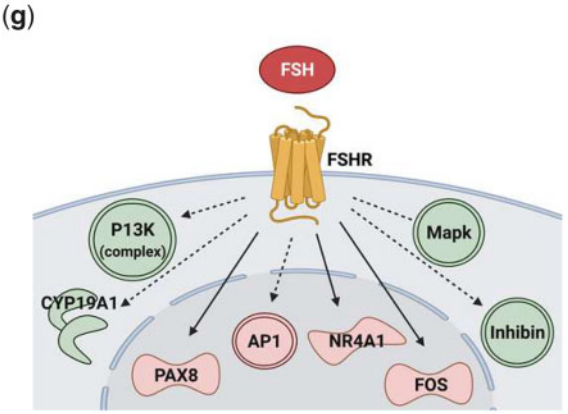

Figure 3. Bioinformatics analysis of early ovarian response genes induced by hypo-glycosylated hFSH18/21 and fully glycosylated hFSH24. Mice were treated for 2 h with Control (PBS), hypo-glycosylated FSH (hFSH18/21) or fully-glycosylated FSH (hFSH24). Ovaries were isolated and processed for RNA-sequencing. (**a**) Principal component analysis (PCA) of the RNA-sequencing data of ovaries. (**b**) Upregulated and downregulated genes in response to FSH18/21 versus Control, FSH24 versus Control and FSH18/21 versus FSH24. (**c**) Venn diagram showing the number of common or differentially expressed ovarian genes between FSH18/21 versus Control, FSH24 versus Control and FSH18/21 versus FSH24. (**d**) Analysis of top 5 molecular and cellular functions determined by Ingenuity pathway analysis (IPA) for FSH18/21 versus Control treatment (top) and FSH24 versus Control treatment (bottom) groups. Red text indicates the unique pathways in each group. (**e**) Top 5 molecular and cellular

the regulation of granulosa cell growth were also rapidly upregulated within 2 h, e.g. the cell cycle marker *Ccnd2* (Supplementary Fig. S8), indicating that FSH18/21 is more likely to stimulate granulosa cell growth *in vivo*.

To investigate the interactions among DEGs, PPI networks for the DEGs in hFSH18/21 versus hFSH24 groups were constructed (Supplementary Fig. S7b). The PPI network consisted of 16 hub genes and 14 interactions (degree > 2). To examine the biological functions of the identified DEGs, functional enrichment of GO pathways was conducted (Supplementary Table SV). The top enriched GO Processes included transcription, and response to the external/endogenous stimulus and hormone. The most enriched GO Function was related to DNA-binding transcription factor activity, with the transcription factor AP-1 complex as the top enriched GO Component. To further confirm the result, the top 50 DEGs between hFSH18/21 and hFSH24 (Supplementary Fig. S7) were selected and the STRING PPI database was used for network connectivity analysis (Supplementary Fig. S9a). Enrichment analysis revealed *Transcription Factor AP-1 Complex* (GO: 0035976) as the only significantly enriched (FDR = 0.0115) GO Cellular Component term (Supplementary Fig. S9b).

GO pathway analysis showed significant differences in DNA binding and transcriptional regulation between hFSH18/21 and hFSH24 treatments (Supplementary Table SV). A very large proportion of DNA-interacting proteins (~1500) are presumed to act as transcription factors (Lambert *et al.*, 2018). Therefore, we compared the expression of 34 transcription factors in each group (Fig. 4). Early growth response 1 and 2 (*Egr1* and *Egr2*) were both significantly upregulated in the hFSH18/21 group compared with control or hFSH24 groups (Fig. 4b). The expression level of nuclear receptor 4a1 (*Nr4a1*) was also highly upregulated in the hFSH18/21 group compared with Control and/or FSH24 treatment (Fig. 4c). However, there were no significant differences in either *Nfkb1* or *Nfkb2* transcript levels between the hFSH18/21 and hFSH24 treatment groups (Fig. 4d). The activator protein-1 (AP-1) transcription factor family consists of a number of members including FOS and JUN. The expression levels of *Fos*, *Jun* and *Junb* were significantly upregulated in the hFSH18/21 group compared with hFSH24 treatment (Fig. 4e and f). Both hFSH18/21 and hFSH24 stimulated the expression of *Jund* and *Fosb*, although no statistical differences were observed between treatments.

Hypo-glycosylated recombinant FSH more efficiently stimulates multiple RTKs and their downstream MAPK/ERK and PI3K/AKT pathways

Multiple RTKs are involved in the regulation of folliculogenesis (Hsueh *et al.*, 2015). To understand the ability of FSH glycoforms to stimulate RTKs activity *in vivo*, a mouse Proteome Profiler Phospho-RTK Array including 39 RTKs was used to evaluate the protein pools derived from ovaries from 5 mice in each of 3 treatment groups (Control, hFSH18/21 and hFSH24; 2 h after treatment). These results showed that multiple RTKs were activated within 2 h by FSH glycoforms, including EGFR, FGFR, Insulin R/IGFR, PDGFR, NGFR, and VEGFR, *etc.* (Supplementary Figs S10 and S11). EGFR (Fig. 5a) and FGFR signaling (Fig. 5b) are 2 of the abundant signals of the RTKs activated by FSH. Western blot was performed to validate the effects of FSH on RTKs and downstream signaling molecules (Fig. 5c). Based on western blotting with phospho-specific EGFR and FGFR antibodies, hFSH18/21 significantly activated EGFR and FGFR (Supplementary Fig. S12a and b). The common signaling pathways induced by FSH and each of these RTK pathways are PI3K/AKT and MAPK/ERK and both were significantly activated in response to hFSH18/21 treatment when compared with FSH24 (Fig. 5e, Supplementary Fig. S12c–e). Furthermore, FSH18/21 stimulated p-P70S6K, which has been implicated in the actions of FSH on follicle growth (Musnier *et al.*, 2009) (Supplementary Fig. S12f). The activation of p-P70S6K and p-p44/42 MAPK stimulated by different FSH glycoforms were confirmed in primary cultured human granulosa cells (Fig. 5d). AP-1 was also significantly activated in the FSH18/21 treatment group as indicated by the phosphorylation of JUN (Supplementary Fig. S12h).

MAPK/ERK and PI3K/AKT pathways are involved in FSH induced follicle growth

FSH activates multiple signaling pathways in the follicle (Landomiel *et al.*, 2019; Johnson and Jonas 2020). An *in vitro* ovarian culture system was used to examine the roles of MAPK/ERK and PI3K/AKT signaling during FSH-induced follicular growth. Wedge sections of mouse ovaries were pretreated for 1 h in the presence or absence of selective inhibitors of PI3K (Wortmannin) or MEK (U0126) before culturing for 48 h with hFSH18/21 or hFSH24. Transcripts for the cell proliferation marker *Pcna* were clearly induced in response to hFSH18/21 but not hFSH24 (Fig. 6a, upper panel). The stimulatory responses to FSH21/24 on *Pcna* expression were abrogated by pretreatment with the MEK inhibitor (Fig. 6a) or the PI3K inhibitor (Fig. 6d). A high *Bcl2* to *Bax* ratio is indicative of follicle health. Like previous *in vivo* observations (Figs 1 and 2), *in vitro* treatment with hFSH18/21 but not hFSH24 (Fig. 6b) induced a favorable ratio of *Bcl2/Bax* expression. The response to FSH18/21 was prevented by pretreatment with either inhibitor (Fig. 6b and e). Treatment with FSH18/21 had reduced levels of *Caspase 3* transcripts compared to treatment with FSH24 (Fig. 6c). Apoptosis-related expression of *Caspase 3* transcripts was increased following treatment with either U0126 (Fig. 6c) or Wortmannin (Fig. 6f). In the Wortmannin treated group, treatment with FSH24 had relatively

Figure 3. Continued
functions determined by IPA between the FSH18/21 versus FSH24 treatment groups. (**f**) Top 5 canonical pathways (absolute Z score > 3.0, -log *P*-value < 1.3, exclude Degradation/Utilization/Assimilation and Disease Specific Pathways) between FSH18/21 versus FSH24 treatment. Red color indicates upregulated genes in each pathway; white color indicates no overlap with dataset. (**g**) Overlay of protein coding DEGs of FSH18/21 versus FSH24 treatment on the FSH pathway using the Path Explorer tool in IPA.

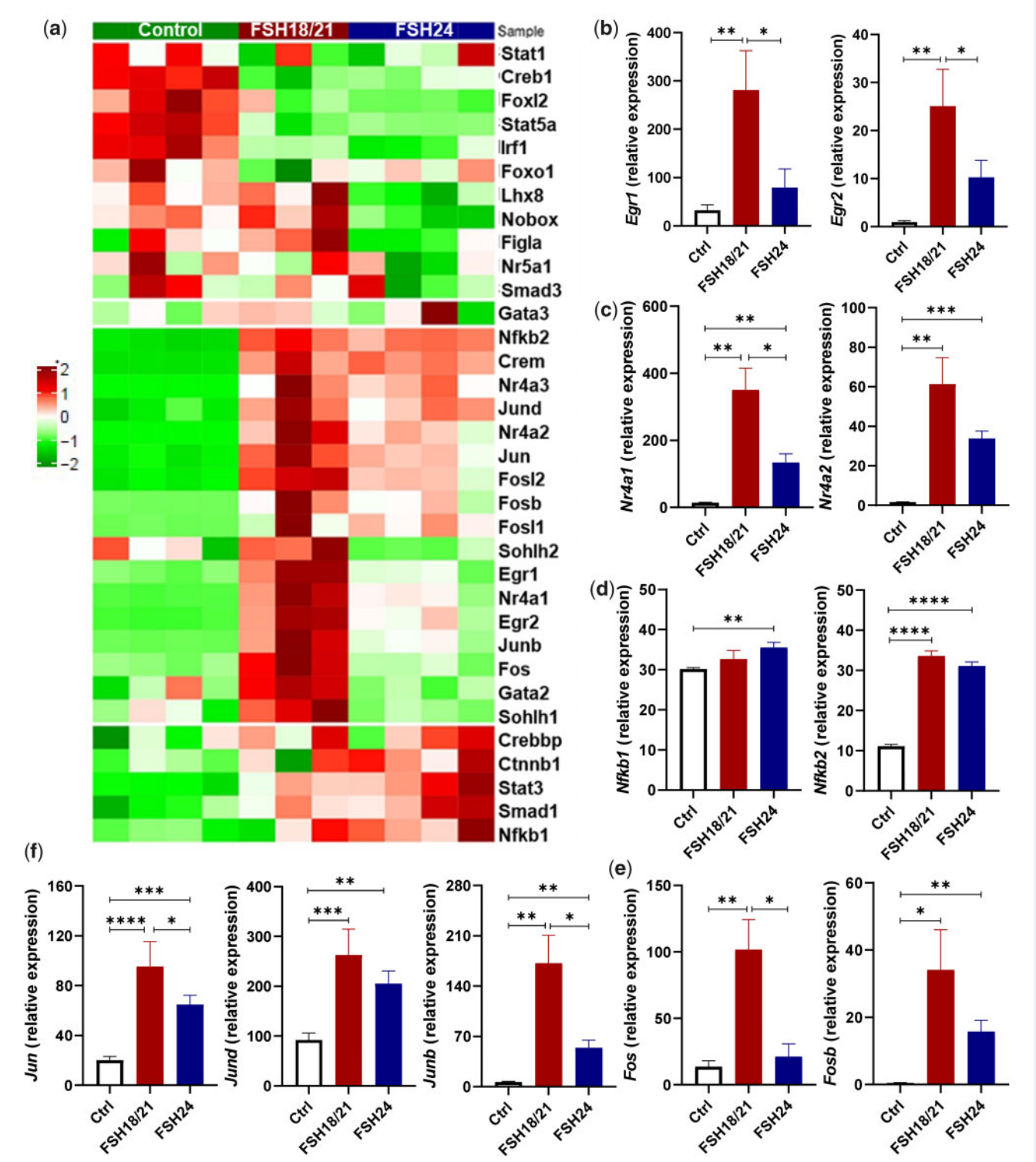

Figure 4. Differential effects of hFSH18/21 and hFSH24 glycoforms on expression of transcription factors. (**a**) Heatmap of transcripts for 34 differentially expressed transcription factors. (**b–e**) Relative expression of groups of transcription factors following treatment with FSH18/21 or FSH24 compared to control. *$P < 0.05$; **$P < 0.01$; ***$P < 0.001$; ****$P < 0.0001$.

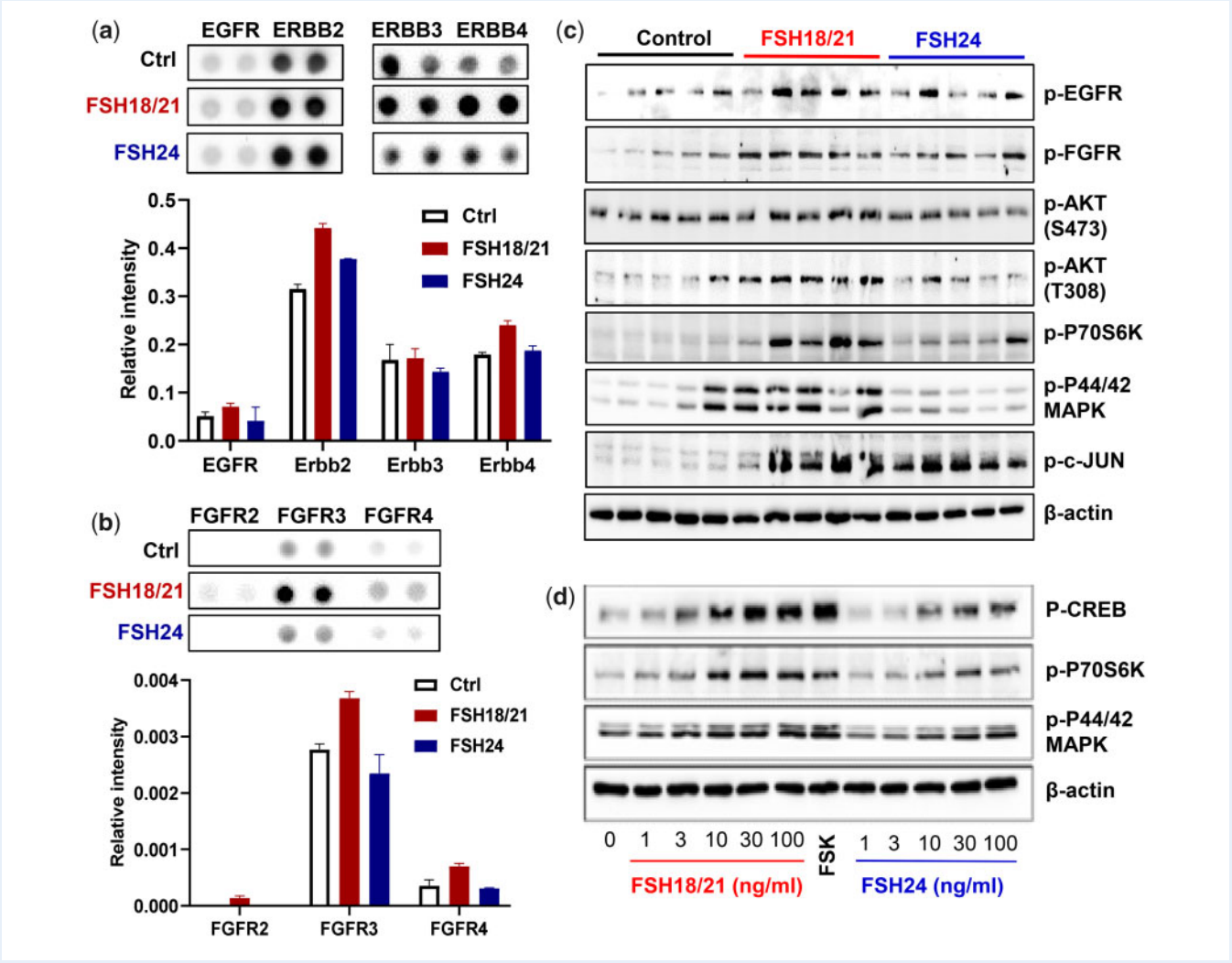

Figure 5. Screening of hypo- and fully-glycosylated human recombinant FSH (hFSH) crosstalk with receptor tyrosine kinase (RTK) signaling and downstream signaling pathways. PND 17 mice (n = 5) were treated i.p. with PBS (Ctrl), or 1 μg of either FSH18/21 or FSH24 for 2 hrs. Ovaries were isolated and total proteins were prepared. (**a**) Total protein pool from each group (n = 5) was used to perform the RTK assay. Selected image of Mouse RTK array showing the differentially activated EGFR signaling responding to the different FSH glycoform treatments (upper panel). Quantification data showing the relative phosphorylation levels of various EGFR family members (lower panel). (**b**) Selected image of the RTK array (upper panel) and quantification data (lower panel) showing the differential activation levels of the FGFR family. The immunosignal intensity was normalized to the control spot on each array. Each bar represents the mean immunosignal intensity ± SEM of duplicates of each RTK. (**c**) Protein extracts from one ovary from each mouse was prepared for Western blot analysis. The image shows the activation of RTKs and downstream pathways. (**d**) Human granulosa cells were treated with increasing concentrations of either FSH18/21 or FSH24 for 30 min. Western blot image showing the activation of pathways in human primary granulosa cells. Forskolin (FSK, 10 μM) was used as positive control.

higher levels of *Caspase 3* transcripts compared with the hFSH18/21 (Fig. 6f).

Half-life and glycan clearance analysis of different FSH glycoforms

Recombinant hFSH18/21 and hFSH24 clearance patterns following intraperitoneal injection (10 μg) revealed differential clearance patterns (Supplementary Fig. S13). FSH18/21 serum concentrations reached a maximum 20 min after i.p. injection, decreased rapidly thereafter, and were 10% of maximum within 3 h and 4% at 4 h. Circulating hFSH24 reached maximum concentrations at 40 min post-injection, remained at that level for an additional 20 min, then decreased slowly to 27% of maximum concentration by 4 h. The area under the curve for hFSH24 was 4 times that of hFSH18/21 ($P < 0.01$, n = 3). When 1 μg samples of both glycoforms were tested, the uptake and clearance patterns were similar, with rapid uptake and disappearance of hFSH18/21 in contrast to prolonged measurable hFSH24 (Supplementary Fig. S13b).

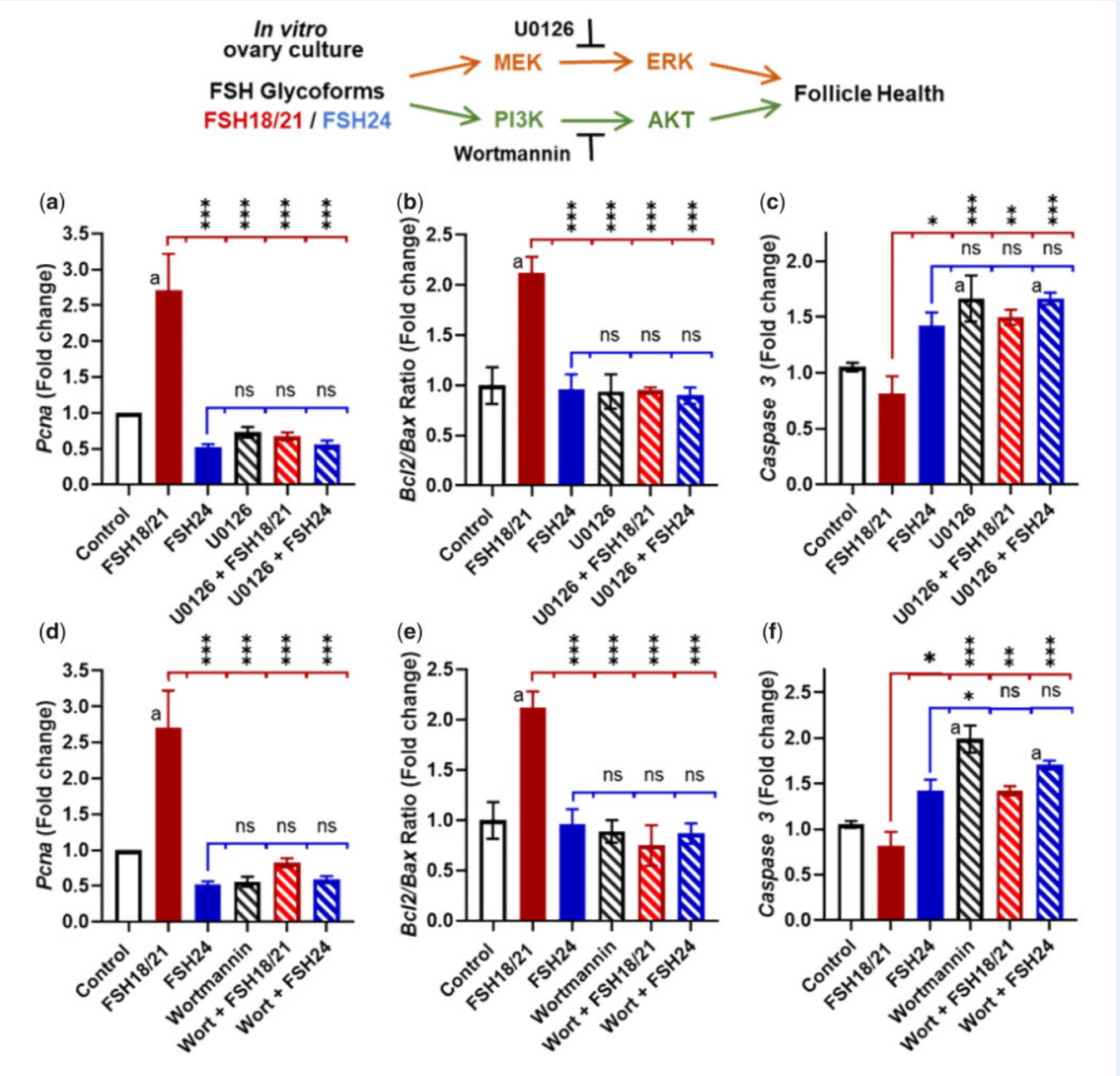

Figure 6. The effect of PI3K and MEK inhibitors on FSH glycoform-dependent regulation of apoptotic and proliferative gene expression in ovarian wedge sections. Ovary sections were pre-treated with either media containing vehicle (Control), 10 μM U0126 (MEK inhibitor) (**a–c**) or 100 nM Wortmannin (Wort, PI3K inhibitor) (**d–f**) for 60 min. Following pre-treatment, ovarian sections were treated with media alone (Control), 30 ng/ml FSH18/21 or FSH24. Ovary wedge sections were snap-frozen and analyzed by quantitative RT-PCR. (**a** and **d**) Proliferating cell nuclear antigen (*Pcna*) gene expression is increased in ovary wedge sections treated with FSH18/21. (**b** and **e**) *Bcl2/Bax* ratio of ovary wedge sections, a high *Bcl2* to *Bax* ratio is indicative of follicle health as seen in the FSH18/21 treatment group. (**c** and **f**) Apoptosis related expression of *Caspase3* transcripts is increased following treatment with Wortmannin and U0126. Ovarian sections treated with FSH18/21 expressed reduced levels of *Caspase 3* transcripts compared to sections treated with FSH24. Data was analyzed using one-way ANOVA with Dunnett's *post hoc* test. Bars represent means ± SEM for six individual ovarian wedge sections. Bars marked [a] indicate a significant difference from Control (open bar). Comparisons among indicated treatments, $^{*}P < 0.05$, $^{**}P < 0.01$, $^{***}P < 0.001$.

Discussion

Since the first IVF baby was born in 1982, it is estimated that more than 400,000 babies from 1.6 million ART cycles are born around the world every year (Sadeghi 2018). Patient response to exogenous hormone stimulation is the first critical step that determines whether IVF clinics achieve a successful outcome. The annual success rate of IVF clinics varies from 10% to 40% (Kushnir *et al.*, 2017). The widely used recombinant FSH preparations employed in ART are largely fully-glycosylated FSH24 (Jiang *et al.*, 2015), which is the predominant FSH glycoform produced in the pituitaries of advanced reproductive age and peri-menopausal women, who experience reduced rates of ART success (van Rooij *et al.*, 2003). By employing an *in vivo* mouse model, our present data clearly show that hypo-glycosylated hFSH, despite its rapid clearance, has greater potential to drive follicular growth *in vivo*. In addition, hypo-glycosylated FSH treatment did not dramatically influence circulating estradiol levels when compared with fully-glycosylated FSH. The observation of enhanced follicle growth without exaggerated estradiol production may be useful clinically because overstimulation of follicle development and elevated estradiol levels may lead to lower endometrial receptivity and thus reduced pregnancy rates (Khalaf *et al.*, 2000; Ocal *et al.*, 2004), as well as increasing the risk of underweight infants, and preeclampsia (Imudia *et al.*, 2012).

Apoptosis of patient follicle granulosa cells is among the factors that will determine IVF outcomes (Baka and Malamitsi-Puchner, 2006). Low levels of apoptotic cells are associated with better fertilization rates and higher-quality embryos (Høst *et al.*, 2000; Regan *et al.*, 2018). The Bax protein is more abundant in granulosa cells of atretic follicles, whereas the Bax protein is extremely low in healthy follicles (Kugu *et al.*, 1998). Our findings demonstrate that fully-glycosylated hFSH24 induces a significantly higher pro-apoptotic index (Bax/Bcl2 ratio) than hFSH18/21. Immunofluorescence staining further supports this idea, showing that granulosa cells of mice treated with fully-glycosylated FSH also displayed elevated cleaved caspase 3, another pro-apoptotic marker. Furthermore, hypo-glycosylated FSH also exhibited greater activity in enhancing follicle growth and maintaining granulosa cell survival compared with control or fully-glycosylated FSH *in vivo* and in an *in vitro* ovarian culture system. The anti-apoptotic actions of FSH, in addition to direct intracellular actions, could be mediated by estradiol and other growth factors/hormones (Regan *et al.*, 2018). Our data show that hypo-glycosylated FSH induced significantly higher levels of serum estradiol compared with control, while no significant difference was found between fully-glycosylated FSH and the control group. Collectively, these data indicate that estradiol increases in response to hypo-glycosylated FSH may promote healthy follicle development.

Previous studies identified a number of FSH responsive genes in various model systems, including human (Perlman *et al.*, 2006), bovine (Sugimura *et al.*, 2017; Nivet *et al.*, 2018), porcine (Liang *et al.*, 2020) and avian granulosa cells (Du *et al.*, 2018). However, little is known about the early induction of networks of genes induced by FSH glycoforms *in vivo*. In the present study, global ovarian transcriptomics showed that in addition to the traditional cAMP signaling (Riccetti *et al.*, 2018), hypo-glycosylated FSH18/21 provokes much greater expression of early response genes after 2 h compared with control and fully-glycosylated FSH. This finding is consistent with our previous *in vitro* study showing that FSH18/21 binds and activates FSHRs more rapidly than FSH24 (Bousfield *et al.*, 2014a). The ability to induce expression of multiple DNA binding transcription factors may be important for the greater ability of hFSH18/21 to induce follicular development compared to hFSH24. Prominent among the transcription factors is the activator transcription factor AP-1 complex (FOS/JUN family), which has been implicated in cellular proliferation, differentiation, transformation, follicular development, ovulation and luteal formation (Rodríguez-Berdini *et al.*, 2020). FSH stimulates expression of multiple AP-1 family genes in *in vitro* cultures of ovarian granulosa cells via Gs/cAMP/PKA-mediated signaling, including *Junb*, *Jun*, *Fos* and *Fra2* (Sharma and Richards, 2000). Research from the Eppig laboratory (Wigglesworth *et al.*, 2015) revealed that *Fos*, *Fosb*, *Jun*, and *Junb* transcripts expressed at higher levels in cumulus cells versus mural granulosa cells of both small and large antral follicles from mouse ovaries treated with eCG. Besides, the induction of transcripts for *Egr* and *Btg* family members, which were expressed at higher levels in mice treated with FSH18/21 compared to FSH24, are important for follicular development and the ovulatory response (Espey *et al.*, 2000; Russell *et al.*, 2003; Sayasith *et al.*, 2006; Hou *et al.*, 2008). Taken together, all these data suggested that FSH18/21 has greater ability to drive expression of early response genes correlated with follicular development and differentiation.

Crosstalk of GPCRs like gonadotropin receptors with RTKs are intrinsically linked to folliculogenesis (El-Hayek *et al.*, 2014) and ovulation (Hsieh *et al.*, 2007). Further, FSH can stimulate tyrosine kinase receptor (RTK) signaling with or without activating the PKA pathway in granulosa cells (Sharma and Richards, 2000; Wayne *et al.*, 2007; Gloaguen *et al.*, 2011). Our study indicated that hFSH18/21 and hFSH24 have differing abilities to activate RTKs *in vivo*, such as EGFR, FGFR, *etc.* RTK activation leads to the recruitment of scaffold proteins, in addition to downstream activation of MAPK and PI3K (Wayne *et al.*, 2007).

The PI3K/AKT and MAPK/ERK signaling pathways are involved in the regulation of follicle development (Donaubauer *et al.*, 2016; Grosbois and Demeestere, 2018). In addition, two of the central signaling pathways activated by FSH via PKA are PI3K/AKT and MAPK/ERK (Casarini and Crepieux, 2019). Furthermore, canonical PKA-dependent (Riccetti *et al.*, 2018) and PKB/AKT signaling are required for full FSH biological activity (Wayne *et al.*, 2007). PI3K/mTOR/p70S6K signaling plays an important role in FSH-induced actions including proliferation, gene transcription, and protein translation (Gloaguen *et al.*, 2011). FSH can also activate MAPK/ERK signaling in a PKA-dependent or PKA-independent manner (Donaubauer *et al.*, 2016; Kahnamouyi *et al.*, 2018). Our short-term *in vivo* data document that FSH18/21 rapidly stimulates both PI3K/AKT/p70S6K and MAPK/ERK pathways.

Taken together, our current study indicates that, hFSH18/21, when compared with hFSH24, has greater bioactivity to promote follicular development *in vivo*, and rescue follicle granulosa cell apoptosis both *in vivo* and *in vitro*. Hypo-glycosylated FSH, which has higher FSHR binding affinity (Bousfield *et al.*, 2014a), by either activation of PKA (Jiang *et al.*, 2015; Liang *et al.*, 2020) or activation of multiple RTKs, more effectively stimulates PI3K/AKT and MAPK/ERK signaling, which is required for optimal follicular development. In addition, hypo-glycosylated FSH stimulates greater induction of early response transcription factors, especially AP-1 and EGR factors, which can promote gene expression related with follicular growth. Evidence in the present study suggests the potential of hypo-glycosylated FSH application in clinical ART.

Supplementary data

Supplementary data are available at *Human Reproduction* online.

Data availability

The data underlying this article will be shared on reasonable request to the corresponding author.

Acknowledgements

We appreciate the University of Virginia Center for Research in Reproduction Ligand Assay and Analysis Core for estradiol and AMH analysis (NICHD P50-HD28934). We thank the Bioinformatics and Systems Biology Core, the Nebraska DNA Sequencing Core, and the Advanced Microscopy Core Facility at UNMC, which receive partial support from the Nebraska Research Initiative and NIGMS INBRE (P20GM103427) and the Fred & Pamela Buffett Cancer Center Support Grant (5P30CA036727).

Authors' roles

GH performed the study, conducted data analysis, and wrote the manuscript; JG, KC, XH, and HRB contributed to experimental methods and edited the manuscript; KCJ, GPJ performed the *in vitro* ovary studies and edited the manuscript; VYB, JVM and GRB prepared hFSH glycoforms: ARB, SK, JVM and GRB performed the FSH clearance study and edited the manuscript; SS, CG, JE performed RNAseq and bioinformatics analysis; XH prepared the human GCs; JSD developed the project, provided resources, supervised the study, revised and edited the manuscript.

Funding

This work was supported by NIH 1P01 AG029531, NIH 1R01 HD 092263, VA I01 BX004272, and the Olson Center for Women's Health. JSD is the recipient of a VA Senior Research Career Scientist Award (1IK6 BX005797). This work was also partially supported by National Natural Science Foundation of China (No. 31872352).

Conflict of interest

The authors declare that there are no conflicts of interests.

References

Allan CM, Wang Y, Jimenez M, Marshan B, Spaliviero J, Illingworth P, Handelsman DJ. Follicle-stimulating hormone increases primordial follicle reserve in mature female hypogonadal mice. *J Endocrinol* 2006;**188**:549–557.

Baka S, Malamitsi-Puchner A. Novel follicular fluid factors influencing oocyte developmental potential in IVF: a review. *Reprod Biomed Online* 2006;**12**:500–506.

Bousfield GR, Butnev VY, Butnev VY, Hiromasa Y, Harvey DJ, May JV. Hypo-glycosylated human follicle-stimulating hormone (hFSH(21/18)) is much more active *in vitro* than fully-glycosylated hFSH (hFSH(24)). *Mol Cell Endocrinol* 2014a;**382**:989–997.

Bousfield GR, Butnev VY, Rueda-Santos MA, Brown A, Hall AS, Harvey DJ. Macro-and micro-heterogeneity in pituitary and urinary follicle-stimulating hormone glycosylation. *J Glycomics Lipidomics* 2014b;**4**:1000125.

Bousfield GR, Butnev VY, Walton WJ, Nguyen VT, Huneidi J, Singh V, Kolli VSK, Harvey DJ, Rance NE. All-or-none N-glycosylation in primate follicle-stimulating hormone β-subunits. *Mol Cell Endocrinol* 2007;**260–262**:40–48.

Bousfield GR, Harvey DJ. Follicle-stimulating hormone glycobiology. *Endocrinology* 2019;**160**:1515–1535.

Bousfield GR, May JV, Davis JS, Dias JA, Kumar TR. *In vivo* and *in vitro* impact of carbohydrate variation on human follicle-stimulating hormone function. *Front Endocrinol* 2018;**9**:216.

Butnev VY, Butnev VY, May JV, Shuai B, Tran P, White WK, Brown A, Smalter Hall A, Harvey DJ, Bousfield GR *et al.* Production, purification, and characterization of recombinant hFSH glycoforms for functional studies. *Mol Cell Endocrinol* 2015;**405**:42–51.

Casarini L, Crepieux P. Molecular mechanisms of action of FSH. *Front Endocrinol (Lausanne)* 2019;**10**:305.

Davis JS, Kumar TR, May JV, Bousfield GR. Naturally occurring follicle-stimulating hormone glycosylation variants. *J Glycomics Lipidomics* 2014;**4**:e117.

Daya S, Gunby J. Recombinant versus urinary follicle stimulating hormone for ovarian stimulation in assisted reproduction. *Hum Reprod* 1999;**14**:2207–2215.

Donaubauer EM, Law NC, Hunzicker-Dunn ME. Follicle-stimulating hormone (FSH)-dependent regulation of extracellular regulated kinase (ERK) phosphorylation by the mitogen-activated protein (MAP) kinase phosphatase MKP3. *J Biol Chem* 2016;**291**:19701–19712.

Du L, Gu T, Zhang Y, Huang Z, Wu N, Zhao W, Chang G, Xu Q, Chen G. Transcriptome profiling to identify key mediators of granulosa cell proliferation upon FSH stimulation in the goose (Anser cygnoides). *Br Poult Sci* 2018;**59**:416–421.

El-Hayek S, Demeestere I, Clarke HJ. Follicle-stimulating hormone regulates expression and activity of epidermal growth factor receptor in the murine ovarian follicle. *Proc Natl Acad Sci USA* 2014;**111**:16778–16783.

Espey LL, Ujioka T, Russell DL, Skelsey M, Vladu B, Robker RL, Okamura H, Richards JS. Induction of early growth response protein-1 gene expression in the rat ovary in response to an ovulatory dose of human chorionic gonadotropin. *Endocrinology* 2000;**141**:2385–2391.

Francois CM,2PetitF,2GitonF,2GougeonA,2RavelC,2MagreS,2Cohen-TannoudjiJ,2GuigonCJ. A novel action of follicle-stimulating hormone in the ovary promotes estradiol production without inducing excessive follicular growth before puberty. *Sci Rep* 2017;**7**:46222.

George JW, Dille EA, Heckert LL. Current concepts of follicle-stimulating hormone receptor gene regulation. *Biol Reprod* 2011;**84**:7–17.

Glanowska KM, Burger LL, Moenter SM. Development of gonadotropin-releasing hormone secretion and pituitary response. *J Neurosci* 2014;**34**:15060–15069.

Gloaguen P, Crépieux P, Heitzler D, Poupon A, Reiter E. Mapping the follicle-stimulating hormone-induced signaling networks. *Front Endocrinol (Lausanne)* 2011;**2**:45.

Grosbois J, Demeestere I. Dynamics of PI3K and Hippo signaling pathways during *in vitro* human follicle activation. *Hum Reprod* 2018;**33**:1705–1714.

Høst E, Mikkelsen AL, Lindenberg S, Smidt-Jensen S. Apoptosis in human cumulus cells in relation to maturation stage and cleavage of the corresponding oocyte. *Acta Obstet Gynecol Scand* 2000;**79**: 936–940.

Hou X, Arvisais EW, Jiang C, Chen D-B, Roy SK, Pate JL, Hansen TR, Rueda BR, Davis JS. Prostaglandin F2alpha stimulates the expression and secretion of transforming growth factor B1 via induction of the early growth response 1 gene (EGR1) in the bovine corpus luteum. *Mol Endocrinol* 2008;**22**:403–414.

Hsieh M, Lee D, Panigone S, Horner K, Chen R, Theologis A, Lee DC, Threadgill DW, Conti M. Luteinizing hormone-dependent activation of the epidermal growth factor network is essential for ovulation. *Mol Cell Biol* 2007;**27**:1914–1924.

Hsueh AJW, Kawamura K, Cheng Y, Fauser BCJM. Intraovarian control of early folliculogenesis. *Endocr Rev* 2015;**36**:1–24.

Hua G, He C, Lv X, Fan L, Wang C, Remmenga SW, Rodabaugh KJ, Yang L, Lele SM, Yang P *et al*. The four and a half LIM domains 2 (FHL2) regulates ovarian granulosa cell tumor progression via controlling AKT1 transcription. *Cell Death Dis* 2016;**7**:e2297.

Imudia AN, Awonuga AO, Doyle JO, Kaimal AJ, Wright DL, Toth TL, Styer AK. Peak serum estradiol level during controlled ovarian hyperstimulation is associated with increased risk of small for gestational age and preeclampsia in singleton pregnancies after *in vitro* fertilization. *Fertil Steril* 2012;**97**:1374–1379.

Jiang C, Hou X, Wang C, May JV, Butnev VY, Bousfield GR, Davis JS. Hypoglycosylated hFSH has greater bioactivity than fully glycosylated recombinant hFSH in human granulosa cells. *J Clin Endocrinol Metab* 2015;**100**:E852–E60.

Johnson GP, Jonas KC. Mechanistic insight into how gonadotropin hormone receptor complexes direct signalingdagger. *Biol Reprod* 2020;**102**:773–783.

Kahnamouyi S, Nouri M, Farzadi L, Darabi M, Hosseini V, Mehdizadeh A. The role of mitogen-activated protein kinase–extracellular receptor kinase pathway in female fertility outcomes: A focus on pituitary gonadotropins regulation. *Ther Adv Endocrinol Metab* 2018;**9**:209–215.

Khalaf Y, Taylor A, Braude P. Low serum estradiol concentrations after five days of controlled ovarian hyperstimulation for *in vitro* fertilization are associated with poor outcome. *Fertil Steril* 2000;**74**: 63–66.

Kugu K, Ratts VS, Piquette GN, Tilly KI, Tao X-J, Martimbeau S, Aberdeen GW, Krajewski S, Reed JC, Pepe GJ *et al*. Analysis of apoptosis and expression of bcl-2 gene family members in the human and baboon ovary. *Cell Death Differ* 1998;**5**:67–76.

Kushnir VA, Barad DH, Albertini DF, Darmon SK, Gleicher N. Systematic review of worldwide trends in assisted reproductive technology 2004–2013. *Reprod Biol Endocrinol* 2017;**15**:6.

Lambert M, Jambon S, Depauw S, David-Cordonnier M-H. Targeting transcription factors for cancer treatment. *Molecules* 2018;**23**: 1479.

Landomiel F, De Pascali F, Raynaud P, Jean-Alphonse F, Yvinec R, Pellissier LP, Bozon V, Bruneau G, Crépieux P, Poupon A *et al*. Biased signaling and allosteric modulation at the FSHR. *Front Endocrinol (Lausanne)* 2019;**10**:148.

Liang A, Plewes MR, Hua G, Hou X, Blum HR, Przygrodzka E, George JW, Clark KL, Bousfield GR, Butnev VY *et al*. Bioactivity of recombinant hFSH glycosylation variants in primary cultures of porcine granulosa cells. *Mol Cell Endocrinol* 2020;**514**:110911.

Lv X, He C, Huang C, Wang H, Hua G, Wang Z, Zhou J, Chen X, Ma B, Timm BK *et al*. Timely expression and activation of YAP1 in granulosa cells is essential for ovarian follicle development. *FASEB J* 2019;**33**:10049–10064.

McDonald R, Sadler C, Kumar TR. Gain-of-function genetic models to study FSH action. *Front Endocrinol (Lausanne)* 2019;**10**:28.

Meher BR, Dixit A, Bousfield GR, Lushington GH. Glycosylation effects on FSH-FSHR interaction dynamics: a case study of different FSH glycoforms by molecular dynamics simulations. *PLoS One* 2015;**10**:e0137897.

Michael SD, Kaplan SB, Macmillan BT. Peripheral plasma concentrations of LH, FSH, prolactin and GH from birth to puberty in male and female mice. *J Reprod Fertil* 1980;**59**:217–222.

Musnier A, Heitzler D, Boulo T, Tesseraud S, Durand G, Lécureuil C, Guillou H, Poupon A, Reiter E, Crépieux P *et al*. Developmental regulation of p70 S6 kinase by a G protein-coupled receptor dynamically modelized in primary cells. *Cell Mol Life Sci* 2009;**66**:3487–3503.

Nakahara K, Saito H, Saito T, Ito M, Ohta N, Sakai N, Tezuka N, Hiroi M, Watanabe H. Incidence of apoptotic bodies in membrana granulosa of the patients participating in an *in vitro* fertilization program. *Fertil Steril* 1997;**67**:302–308.

Nivet A-L, Dufort I, Gilbert I, Sirard M-A. Short-term effect of FSH on gene expression in bovine granulosa cells *in vitro*. *Reprod Fertil Dev* 2018;**30**:1154–1160.

Ocal P, Aydin S, Cepni I, Idil S, Idil M, Uzun H, Benian A. Follicular fluid concentrations of vascular endothelial growth factor, inhibin A and inhibin B in IVF cycles: are they markers for ovarian response and pregnancy outcome? *Eur J Obstet Gynecol Reprod Biol* 2004; **115**:194–199.

Oosterhuis GJ, Michgelsen HW, Lambalk CB, Schoemaker J, Vermes I. Apoptotic cell death in human granulosa-lutein cells: a possible indicator of *in vitro* fertilization outcome. *Fertil Steril* 1998;**70**: 747–749.

Orisaka M, Tajima K, Tsang BK, Kotsuji F. Oocyte-granulosa-theca cell interactions during preantral follicular development. *J Ovarian Res* 2009;**2**:9.

Perlman S, Bouquin T, van den Hazel B, Jensen TH, Schambye HT, Knudsen S, Okkels JS. Transcriptome analysis of FSH and FSH variant stimulation in granulosa cells from IVM patients reveals novel regulated genes. *Mol Hum Reprod* 2006;**12**:135–144.

Plewes MR, Hou X, Zhang P, Liang A, Hua G, Wood JR, Cupp AS, Lv X, Wang C, Davis JS *et al*. Yes-associated protein 1 is required for proliferation and function of bovine granulosa cells *in vitro*. *Biol Reprod* 2019;**101**:1001–1017.

Raisova M, Hossini AM, Eberle J, Riebeling C, Wieder T, Sturm I, Daniel PT, Orfanos CE, Geilen CC. The Bax/Bcl-2 ratio determines the susceptibility of human melanoma cells to CD95/Fas-mediated apoptosis. *J Invest Dermatol* 2001;**117**:333–340.

Regan SLP, Knight PG, Yovich JL, Leung Y, Arfuso F, Dharmarajan A. Granulosa cell apoptosis in the ovarian follicle—a changing view. *Front Endocrinol (Lausanne)* 2018;**9**:61.

Riccetti L, Sperduti S, Lazzaretti C, Casarini L, Simoni M. The cAMP/PKA pathway: steroidogenesis of the antral follicular stage. *Minerva Ginecol* 2018;**70**:516–524.

Rodríguez-Berdini L, Ferrero GO, Bustos Plonka F, Cardozo Gizzi AM, Prucca CG, Quiroga S, Caputto BL. The moonlighting protein c-Fos activates lipid synthesis in neurons, an activity that is critical for cellular differentiation and cortical development. *J Biol Chem* 2020;**295**:8808–8818.

Russell DL, Doyle KMH, Gonzales-Robayna I, Pipaon C, Richards JS. Egr-1 induction in rat granulosa cells by follicle-stimulating hormone and luteinizing hormone: combinatorial regulation by transcription factors cyclic adenosine 3',5'-monophosphate regulatory element binding protein, serum response factor, sp1, and early growth response factor-1. *Mol Endocrinol* 2003;**17**:520–533.

Sadeghi MR. The 40th anniversary of IVF: has ARTs success reached its peak? *J Reprod Infertil* 2018;**19**:67.

Sayasith K, Brown KA, Lussier JG, Doré M, Sirois J. Characterization of bovine early growth response factor-1 and its gonadotropin-dependent regulation in ovarian follicles prior to ovulation. *J Mol Endocrinol* 2006;**37**:239–250.

Saz-Parkinson Z, López-Cuadrado T, Bouza C, Amate J-M. Outcomes of new quality standards of follitropin alfa on ovarian stimulation. *BioDrugs* 2009;**23**:37–42.

Sharma SC, Richards JS. Regulation of AP1 (Jun/Fos) factor expression and activation in ovarian granulosa cells Relation of JunD and Fra2 to terminal differentiation. *J Biol Chem* 2000;**275**:33718–33728.

Simon LE, Liu Z, Bousfield GR, Kumar TR, Duncan FE. Recombinant FSH glycoforms are bioactive in mouse preantral ovarian follicles. *Reproduction* 2019;**158**:517–527.

Sugimura S, Kobayashi N, Okae H, Yamanouchi T, Matsuda H, Kojima T, Yajima A, Hashiyada Y, Kaneda M, Sato K *et al.* Transcriptomic signature of the follicular somatic compartment surrounding an oocyte with high developmental competence. *Sci Rep* 2017;**7**:1–14.

Ulloa-Aguirre A, Zariñán T, Jardón-Valadez E, Gutiérrez-Sagal R, Dias JA. Structure-function relationships of the follicle-stimulating hormone receptor. *Front Endocrinol (Lausanne)* 2018;**9**:707.

van Rooij IAJ, Bancsi LFJMM, Broekmans FJM, Looman CWN, Habbema JDF, Te Velde ER. Women older than 40 years of age and those with elevated follicle-stimulating hormone levels differ in poor response rate and embryo quality in *in vitro* fertilization. *Fertil Steril* 2003;**79**:482–488.

Walton WJ, Nguyen VT, Butnev VY, Singh V, Moore WT, Bousfield GR. Characterization of human FSH isoforms reveals a non-glycosylatedβ-subunit in addition to the conventional glycosylatedβ-subunit. *J Clin Endocrinol Metab* 2001;**86**:3675–3685.

Wang H, May J, Butnev V, Shuai B, May JV, Bousfield GR, Kumar TR. Evaluation of *in vivo* bioactivities of recombinant hypo-(FSH21/18) and fully-(FSH24) glycosylated human FSH glycoforms in Fshb null mice. *Mol Cell Endocrinol* 2016;**437**:224–236.

Wayne CM, Fan H-Y, Cheng X, Richards JS. Follicle-stimulating hormone induces multiple signaling cascades: evidence that activation of Rous sarcoma oncogene, RAS, and the epidermal growth factor receptor are critical for granulosa cell differentiation. *Mol Endocrinol* 2007;**21**:1940–1957.

Wigglesworth K, Lee K-B, Emori C, Sugiura K, Eppig JJ. Transcriptomic diversification of developing cumulus and mural granulosa cells in mouse ovarian follicles. *Biol Reprod* 2015;**92**:23.

Zariñán T, Butnev VY, Gutiérrez-Sagal R, Maravillas-Montero JL, Martínez-Luis I, Mejía-Domínguez NR, Juárez-Vega G, Bousfield GR, Ulloa-Aguirre A. *In vitro* impact of FSH glycosylation variants on FSH receptor-stimulated signal transduction and functional selectivity. *J Endocr Soc* 2020;**4**:bvaa019.